Open-switch Fault Detection in Five-phase Induction Motor Drives using Model Predictive Control

I. Gonzalez-Prieto, M.J. Duran, N. Rios-Garcia, F. Barrero, *Senior Member,IEEE*, C. Martin

***Abstract*- Achieving a self-reconfigurable fault-tolerant control in multiphase machines requires a fast fault detection and localization. Most fault detection techniques inherit the three-phase approach by defining fault indices in a per-phase basis. A recent approach suggests an alternative fault detection mechanism based on vector space decomposition (VSD) variables, but the study is limited to open-phase faults (OPFs) for a six-phase drive that is regulated under field oriented control (FOC). It is known however that *i)* the open-switch faults (OSFs) in the converter are more likely than the OPF in the machine and *ii)* the drive performance in the event of an open-circuit fault is more critical when model predictive control (MPC) is used. This work extends the study of the VSD fault detection method to multiphase machines with different number of phases (five), control strategy (MPC) and type of faults (OPF and OSF). Although experimental results show that MPC misbehaves after the fault occurrence, the fast detection provided by the VSD approach allows a satisfactory transition to post-fault mode of operation.**

***Index Terms* — Five-phase induction motor drives, model predictive control, open-switch fault detection.**

I. INTRODUCTION

The focus on multiphase electric drives has been intensified since the beginning of the 21th century both in industry and academia. The steady increase in the studies and proposals from the scientific community has created a body of knowledge that provides further confidence to replace the three-phase standard in certain applications [1-4]. On the other hand, some companies have adopted the multiphase concept in their latest and emblematic products [5-8]. Both from the research and industrial sides, the enhanced fault tolerance provided by multiphase drives has been highlighted as a key issue. For the sake of example, reliability is a main claim in ultra-high-speed elevators [5], wind energy systems [6], aircraft actuators [7] or ship propulsion systems [8].

Manuscript received April 17, 2017; revised June 1, 2017 and July 31, 2017; accepted August 11, 2017. This work was supported by the Spanish Ministry of Science and Innovation and the European Regional Development Fund under Project ENE2014-52536-C2-1-R.

I. Gonzalez-Prieto, M.J. Duran and N. Rios-Garcia are with the Department of Electrical Engineering, University of Malaga, Malaga, Spain (e-mail: ignaciogp87@gmail.com, mjduran@uma.es and nrg@uma.es).

F. Barrero and C. Martin are with the Department of Electronic Engineering, University of Seville, Seville, Spain (e-mail: fbarrero@us.es and cmartin15@us.es).

As in three-phase drives, the most popular strategy to regulate multiphase drives has been the field oriented control (FOC) both in healthy [3] and faulty modes of operation [4]. This cascaded control approach can successfully handle the speed regulation of multiphase machines with small modifications in the control scheme, providing good current tracking within a proved and well-known control scheme. The main recent competitor of FOC is the finite control-set model predictive control (FCS-MPC or just MPC for simplicity), which is claimed to enhance the transient response and provide high flexibility to include restrictions [9-18]. Even though MPC is a promising approach, it is known to be sensitive to parameter variations [15]. Although the parameter mismatch is typically considered in healthy operation (e.g. due to saturation, thermal or deep-bar effects), a more critical situation is faced in the event of a fault. When an open-circuit appears in the electric drive, the MPC aims to regulate the machine with an incorrect model of the system because it still *does not know* that one phase or switch is inactive. As experimentally shown in [16, 17], this results in a poor regulation of the motor until the control is reconfigured in post-fault mode. In other words, the impact of the fault detection delay is more critical in MPC than in FOC, and for this reason the fault detection technique to be used together with MPC should be as fast as possible.

The open-circuit faults can be categorized in open-phase faults (OPFs) and open-switch fault (OSFs) [19-30]. The OPFs typically occur when the machine windings are damaged or there is a disconnection between the voltage source converter (VSC) and the machine. On the other hand, the OSFs are related to converter faults (switch, driver) that leave the upper or lower power switch of a converter leg in open-circuit. While in OPFs the current of the faulty phase cannot flow, in single OSFs the phase current is distorted for half a fundamental period. Nevertheless, in both OPFs and OSFs situations the required action would be the same: the isolation of the faulty phase and the control reconfiguration to operate with the remaining healthy phases. There is consequently no need to distinguish and classify the faults, but it is necessary to use a fault detection method that successfully informs about any kind of open-circuit fault in a robust and quick manner.

For diagnosis purposes, the faults can be detected with a relatively long delay (more than one fundamental period [19-20]) and it is interesting to detect inter-turn faults that can identify the malfunctioning operation in an early stage [31-34]. Different works based on current signature are available in literature for this purpose. Nevertheless, when the aim is to create a self-reconfigurable fault-tolerant multiphase

drive, the focus is typically placed on open-circuit faults, either in the form of open-phase or open-switch types. In such a case the fault detection technique should ideally possess the following features [21]: 1) a short detection time, 2) capability to localize the fault, 3) use of non-invasive techniques, 4) avoid additional hardware, 5) avoid complex approaches with an elevated computational cost, and 6) be independent of the machine parameter, control strategy and operation condition. These characteristics are found in the methods that follow the so-called Park vector approach in three-phase drives [22-25]. Since these methods are per-phase in essence, they can be applied in multiphase systems with good performance.

Most of the fault detection techniques that have been specifically designed for five-phase systems still follow a phase-current-based approach [29-30, 35]. In this way, [30] does not take advantage of the additional degrees of freedom existing in multiphase drives and it is not focused on obtaining a short detection time to help the transition to the post-fault mode. The approach in [27] and [35] is again based on phase currents and it is model-based estimations. This results in a higher complexity and some degree of dependence on both the drive parameters and the operating point.

It is possible however to take advantage of some specific feature in multiphase drives to define fault detection indices based in the VSD components [1-4]. This approach is followed in [27-28] for OSF fault detection and in [21] for OPF detection. Even though both works share the idea of using an VSD approach, the methods are of a very different nature. The method in [27-28] identifies the reference directions in the *x-y* plane and follows a centroid-based approach for the OSFs, and follow a phase-current-based approach for the OPFs. It is generally valid for non-sinusoidal phase current waveforms, but it requires different indices for OSFs and OPFs, and its effectivity is not proven for two open-circuit faults in different legs. On the other hand, [21] is aimed for sinusoidal phase currents, but the same indices are valid for all kind of open-circuit fault (including OPFs and OSFs), is computationally simpler and it is valid for single and multiple open-circuit faults.

The approach in [21] recently proved to outperform the Park vector method in [22], but it has only been tested for specific types of faults (OPFs), number of phases (six) and control strategies (FOC). This works aims to extend and complete the analysis with the following differences:

- *Open-switch faults (OSFs).* It is experimentally confirmed that the VSDFD method can successfully detect all kind of open-circuit faults, including OPFs and OSFs. This is of paramount importance because converter faults are most commonly found in practice.
- *Five-phase system.* The VSDFD is tested in a system with a different phase number, thus confirming the universality of the approach. Fault detection indices are redefined for this specific drive configuration, but the method proves to be equally applicable.
- *Model predictive control (MPC).* The evolution of the phase currents after the open-circuit fault is dependent on the control strategy. This work shows that the VSDFD method can also be applied together with MPC, this being the most critical case since the MPC is known to lose the speed control after the fault occurrence [16-17, 36].

These differences confirm that the VSDFD method can be used regardless of the type of multiphase drive, fault scenario and control strategy. Experimental results confirm the high speed of detection provided by the VSDFD approach and this in turn allows a satisfactory transition from pre- to post-fault mode of operation even using the sensitive MPC strategy. The application of the VSDFD method together with any of the fault-tolerant control strategies suggested in [16, 17, 37-45] provides an electric drive with self-healing properties. This automatic fault tolerance without additional hardware is expected to have industrial use in applications where reliability is a main concern.

II. Finite Control-Set Model Predictive Control of Five-Phase Induction Motor Drives

Before the model predictive control is derived, it is necessary to firstly necessary to consider the system model and characteristics. The topology of the drive under study consists of a five-phase induction machine (IM) supplied from a two-level IGBT-based VSC, as shown in Fig. 1. The machine is assumed to have distributed windings that are symmetrically shifted (θ =72 electrical degrees). Consequently, all spatial harmonics are neglected and a purely sinusoidal airgap distribution of the magneto-motive force (MMF) is considered. For control purposes the equations of the machine are typically expressed in VSD variables using the power-invariant generalized Clarke transformation [46]:

$$[T_0]=\frac{2}{5}\begin{bmatrix} 1 & cos\theta & cos2\theta & cos3\theta & \cos 4\theta \\ 0 & sin\,\theta & sin2\theta & sin3\theta & sin\,4\theta \\ 1 & cos2\theta & cos4\theta & cos\theta & cos3\theta \\ 0 & sin2\theta & sin4\theta & \sin\theta & sin3\theta \\ 1/2 & 1/2 & 1/2 & 1/2 & 1/2 \end{bmatrix} \tag{1}$$

$$\left[i_{\alpha s}\; i_{\beta s}\; i_{xs}\; i_{ys}\; i_{zs}\right]^T=[T_0]\left[i_{as}\; i_{bs} i_{cs}\; i_{ds}\; i_{es}\right]^T$$

This transformation provides the relationship between phase and VSD variables (i.e. *αβxyz*) and it will be the key to later on obtain the fault indices.

Applying standard assumptions, the model of the five-phase induction machine in VSD variables is obtained in (2), where L_s=L_{ls}+M, L_r=L_{lr}+M, M=$5/2\cdot L_m$ and $\omega_r=p\cdot\omega_m$, being p the pole pairs number and ω_m the mechanical speed. Subscripts s and r indicate stator and rotor variables, while subscripts l and m denote leakage and magnetizing inductance, respectively.

$$\begin{aligned} v_{\alpha s} &= \left(R_s+L_s\frac{d}{dt}\right)i_{\alpha s}+M\,\frac{di_{\alpha r}}{dt} \\ v_{\beta s} &= \left(R_s+L_s\frac{d}{dt}\right)i_{\beta s}+M\,\frac{di_{\beta r}}{dt} \\ v_{xs} &= \left(R_s+L_s\frac{d}{dt}\right)i_{xs} \\ v_{ys} &= \left(R_s+L_s\frac{d}{dt}\right)i_{ys} \\ 0 &= \left(R_r+L_r\frac{d}{dt}\right)i_{\alpha r}+M\,\frac{di_{\alpha s}}{dt}+\omega_r L_r i_{\beta r}+\omega_r M i_{\beta s} \\ 0 &= \left(R_r+L_r\frac{d}{dt}\right)i_{\beta r}+M\,\frac{di_{\beta s}}{dt}-\omega_r L_r i_{\alpha r}-\omega_r M i_{\alpha s} \\ T_e &= pM\left(i_{\beta r}i_{\alpha s}-i_{\alpha r}i_{\beta s}\right) \end{aligned} \tag{2}$$

The fault detection technique itself is not model-based, but the predictive approach requires a model of the machine to perform the control, which is obtained from the discretization of (2).

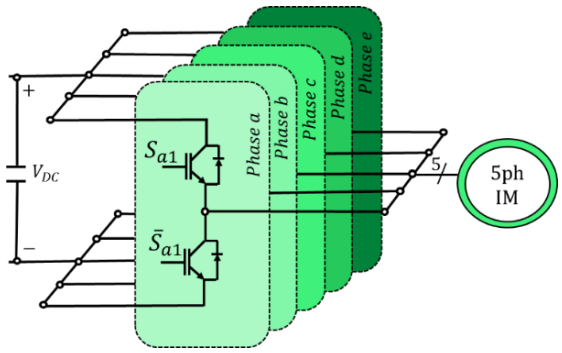

Fig. 1. Scheme of the analyzed five-phase IM drive.

Since a distributed-winding is considered, only α-β components will contribute to the flux and torque production. Conversely, x-y components will only produce stator copper losses. Moreover, if the machine is configured with an isolated neutral, the zero-sequence current i_{zs} will not flow, and consequently these components can be omitted from the analysis.

Finally, to express the machine model in the dq reference frame, where d and q regulate the flux and torque production, respectively, the Park transformation is employed:

$$[D] = \begin{bmatrix} cos\theta_s & sin\theta_s \\ -sin\theta_s & cos\theta_s \end{bmatrix}$$
$$\begin{bmatrix} i_{ds} & i_{qs} \end{bmatrix}^T = [D]\begin{bmatrix} i_{\alpha s} & i_{\beta s} \end{bmatrix}^T \quad (3)$$

where θ_s is the angle of the reference frame and is calculated from the measured speed and the estimated slip [17].

Since the model from (2) is expressed in stationary frame but the current references are provided in d-q components, the rotation from (3) is necessary as the control stage.

The FCS-MPC method can be described as a discrete optimization problem, which selects the control action that minimizes a predefined cost function at each sampling period. This cost function constitutes the control objective. The control structure applied in this work is shown in Fig. 2 and described in [47]. It is based on an outer PI-based speed control loop and an inner current controller using the FCS-MPC technique.

The objective of the FCS-MPC approach is to track the reference stator currents $i^*_{\alpha\beta xy}$. For this purpose, a discrete model of the system (predictive model) is used to estimate the future values of the stator currents $\hat{\imath}_{\alpha\beta xy}$ from the measured phase currents i_s and rotor speed ω_m. This predictive model is obtained from the discretization of the machine's equations (2) using a technique based on the Cayley-Hamilton theorem [14], since this approach has a better precision than the commonly applied Euler method. A prediction is done for each possible voltage vector supplied by the VSC (2^5=32 for the five-phase case) and a cost function J is evaluated. Although there is a high degree of flexibility to define the cost function, the most used control criterion is the minimization of the current error between the reference and the prediction, as follows:

$$J = K_1(i^*_{\alpha s} - \hat{\imath}_{\alpha s})^2 + K_2\left(i^*_{\beta s} - \hat{\imath}_{\beta s}\right)^2 + K_3(i^*_{xs} - \hat{\imath}_{xs})^2 + K_4\left(i^*_{ys} - \hat{\imath}_{ys}\right)^2 \quad (4)$$

where K_i are the weighting factors for each current component, which must be selected according to the control objectives. For the case of distributed-winding machines, the values of these coefficients are selected to obtain a tradeoff between the torque/flux regulation ($K_1$and K_2) and efficiency/distortion (K_3 and K_4). The PI regulator provides the q-current reference while the d-current reference is fixed to a constant value related to the rated flux in the base-speed region. These currents are then rotated to the α-β plane, and x-y currents references are set to zero in healthy operation to minimize the copper losses. Finally, a minimizer selects the optimal control action (switching vector $\bar{S}^{opt}$, where $\bar{S} = [S_a \quad S_b \quad S_c \quad S_d \quad S_e]$) that minimizes the cost function. The optimal gating signal is applied to the VSC during the next sampling instant, being this process repeated every sampling period.

When an open-circuit fault occurs the machine becomes asymmetrical, the voltage in the faulty phase is given by the counter electromotive force (back-EMF) and the number of available voltage vectors is reduced to 2^4=16 [16]. Consequently, the previously described model is no longer valid and a reconfiguration of the controller must be done. However, it is possible to maintain the same equations in VSD variables (2) and in turn limit the changes in the post-fault control scheme by replacing the Clark transformation matrix T_0 by T_p (for the sake of simplicity, phase a is assumed as the faulty phase in the following analysis):

$$[T_p] = \frac{2}{5}\begin{bmatrix} cos\theta - 1 & cos2\theta - 1 & cos3\theta - 1 & \cos 4\theta - 1 \\ sin\,\theta & sin2\theta & sin3\theta & sin\,4\theta \\ sin2\theta & sin4\theta & \sin 6\theta & sin8\theta \\ 1 & 1 & 1 & 1 \end{bmatrix} \quad (5)$$
$$\begin{bmatrix} i_{as} & i_{\beta s} & i_{ys} & i_{zs} \end{bmatrix}^T = [T_p]\begin{bmatrix} i_{bs} i_{cs} & i_{ds} & i_{es} \end{bmatrix}^T$$

The cost function must be correspondingly changed to preserve the optimization criterion.

Taking into account the aforementioned changes, the control scheme from Fig. 2 can be used both in healthy and faulty operation. While the fault detection method informs that the drive is healthy (the fault indices F_k=0), the x-y current references are set null. Once the fault detection stage flags an open-circuit fault (the fault indices F_k=1), the x-y references are set according to the minimum loss or maximum torque criteria detailed in literature [4].

III. Open Circuit Fault Scenarios

This section analyzes different open-circuit fault situations in a multiphase drive (Fig. 3a). The origin of the fault can be either in the machine, the converter or the connection between both. The diverse scenarios lead to four types of different open-circuit faults:

i. *Open-phase fault (OPF):* This term is used in those fault situations where the connection of the machine phase and its corresponding VSC leg is lost. In this type of fault, the current of the affected line cannot flow anymore, and the corresponding post-fault current waveform of that phase is null (see Fig. 3b).

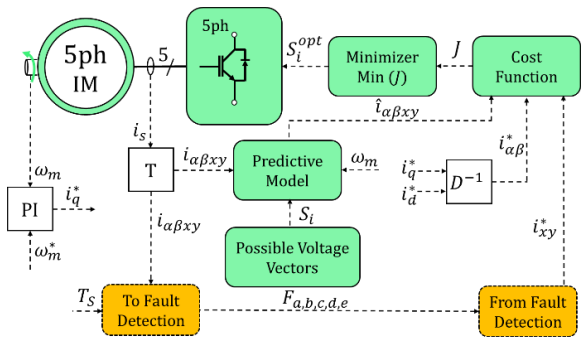

Fig. 2. FCS-MPC scheme for the five-phase IM drive (see Fig. 4 to see the link with the fault detection stage).

ii. Open-circuit fault in the bottom switch (OSF1): This type of fault occurs when the bottom semiconductor $\bar{S}_a$ remains open due to the fault (Fig. 3a). In this situation the current can still flow through the power switch S_a of the faulty phase, but it is limited to zero during the negative cycles (Fig. 3c).

iii. Open-circuit fault in the top switch (OSF2): In this case the top semiconductor S_a is damaged and consequently the situation is opposite to the OSF1 case: the current can flow during the negative part of the cycle but it is limited to zero when the phase current tries to be reversed (see Fig. 3d).

A fourth situation appears when both power switches in the same leg (S_a and $\bar{S}_a$) are open-circuited. In this case the phase is still connected to the VSC and the current can in principle flow through the free-wheeling diodes. However, the current through the faulty phase is essentially null in practice. Since the results of this scenario are mostly similar to those in an open-phase fault, both scenarios are grouped together and they are referred as OPF.

From practical considerations all cases considered above can be derived to an OPF situation (by proper isolation of the phase) and then apply any of the strategies detailed in [16, 17, 37-45]. However, prior to the phase isolation it is necessary to detect and localize all these types of fault scenarios. For this purpose, the next section describes the proposed VSD-based fault detection method.

IV. Description of the Fault Detection Method

While most fault detection methods that are suitable to be applied together with fault-tolerant control strategies are based on phase current monitoring, an improved approach based on VSD variables (named VSDFD) has been recently proposed in [21]. Both in [28] and in the VSDFD of [21] the fault indices that identify the fault occurrence directly depend on the x-y current components. This novel procedure benefits from two interesting characteristics of multiphase machines with distributed windings: *i)* x-y current components are zero in healthy operation and *ii)* they do not contribute to the flux/torque production. Feature *i)* allows an arbitrary setting of the moving average period of integration, while *ii)* guarantees that no false alarms will be obtained as long as the x-y currents are satisfactorily regulated [19].

The procedure to obtain the VSD fault indices is to use the inverse Clarke transformation in (1), set the OPF condition ($i_{ph} = 0$) and then extract from this restriction the corresponding ratio. For the sake of our example where a is the considered faulty phase, the restriction is $-\frac{i_x}{i_\alpha} = 1$, which leads to the following fault index: $R_a = -\frac{i_x}{i_\alpha}$. Note that the process can be generalized for the remaining phases, whose fault indices can be obtained as:

$$\begin{aligned} R_b &= \frac{i_x}{0.38i_\alpha + 1.17 \cdot i_\beta - 0.73 \cdot i_y} \\ R_c &= \frac{i_x}{2.62i_\alpha - 1.90i_\beta + 3.08i_y} \\ R_d &= \frac{i_x}{2.62i_\alpha + 1.90i_\beta - 3.08i_y} \\ R_e &= \frac{i_x}{0.38i_\alpha - 1.17i_\beta - 0.7266i_y} \end{aligned} \tag{6}$$

It is remarkable that these fault indices differ from the ones obtained in [21], as a consequence of using a different type of multiphase machine. However, the procedure for reaching them is exactly the same and can be extended to any multiphase machine. Opposite to the alternating nature of phase currents, the VSD ratios from (6) provide well-defined constant values: zero in healthy condition and one in OPF situation. This is particularly advantageous in order to detect and localize the fault. The normalization of ratios R_k in (6) help the fault detection technique to be independent on the operating point and system parameters. As in Park vector methods, the ratios R_k can be integrated using a moving average:

$$\langle R_k(t) \rangle = \frac{1}{T_m} \int_{t-T_m}^{t} R_k(t)\, dt, \tag{7}$$

but it is not necessary in this case to calculate the absolute value, and the period of the moving average T_m does not need to coincide with the fundamental period T_f. On the contrary, the period T_m can be freely chosen as a certain portion of $\hat{T}_f$:

$$T_m = \sigma \cdot \hat{T}_f \quad \sigma \leq 1, \tag{8}$$

where σ is a parameter that defines the portion of the fundamental period that is used in the moving average. The selection of σ is done to obtain a satisfactory compromise between detection time and fault index noise.

The VSDFD method applies then a hysteresis band to the ratios R_k for noise rejection. In post-fault situation the fault index is one, which is applied to filter all indices using the following hysteresis band:

$$\begin{aligned} &if \quad 1 - \varepsilon \leq R_k \leq 1 + \varepsilon \quad then \; R_k^{pb} = R_k \\ &else \; R_k^{pb} = 0 \end{aligned} \tag{9}$$

The width of the hysteresis band (ε) should be limited in order to ensure a low ripple of the fault indices in the healthy phases.

If the filtered values R_k^{pb} are then averaged as in (7), the new fault indices are:

$$e_k = \int_{t-T_m}^{t} R_k^{pb}(t)\, dt \qquad k \in \{a, b, c, d, e\} \tag{10}$$

And the information of the faulty phases F_k is obtained comparing the fault indices with the threshold:

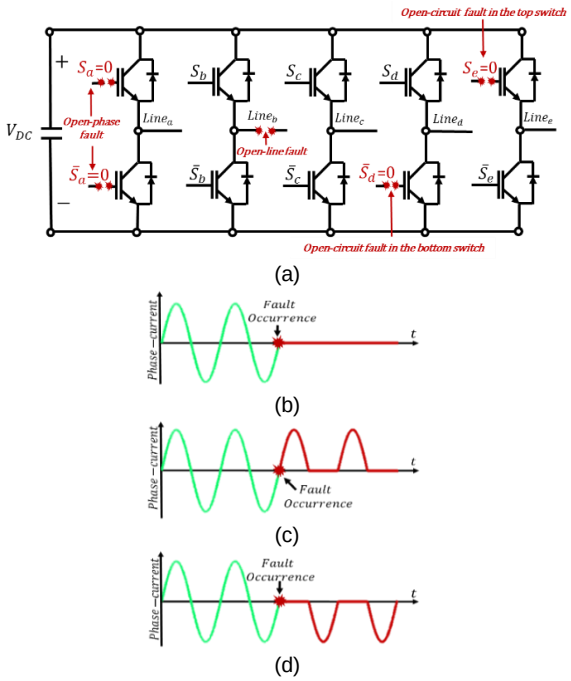

Fig. 3. a) Scheme of a five-phase VSC with different types of faults. b) Current waveform in open-line fault or open-phase fault, c) current waveform in open-circuit fault of the top switch and d) current waveform in open-circuit fault of the bottom switch.

$$if\ e_k \geq T_{th}\ \ then\ F_k = 1$$
$$else\ F_k = 0 \tag{11}$$

From the flag provided by (11), the fault can be finally detected and localized (see Fig. 4). Once this occurs, it is necessary to calculate the new x-y references that need to be provided to the control stage in Fig. 2. These values are taken from existing works [4], completing in this manner the connection between the fault detection (Fig. 4) and post-fault control reconfiguration (Fig. 2) stages. The joint application of fault detection and post-fault control reconfiguration provides a self-reconfigurable fault-tolerant MPC-regulated five-phase induction motor drives.

V. Experimental Results

The aim of this section is to verify that the VSDFD method can successfully detect and localize all kind of open-circuit faults in MPC-based five-phase induction motor drives.

A scheme of the utilized experimental system is shown in the Fig. 5. It is based on a five-phase IM controlled using two three-phase VSI. The controller is implemented in an electronic board based on the MSK28335 using a sampling period of 100 μs. A programmable load torque can be applied to the five-phase IM using a DC machine mechanically coupled to the multiphase drive, while the DC-link voltage is set using an external DC supply to 300 V. The parameters of the custom-built five-phase machine have been determined with ac-time domain and stand-still tests [48-49]. The obtained induction machine parameters are shown in the table I.

Eight tests have been designed to explore the performance of the VSDFD technique (speed of detection, robustness and impact of the fault detection delay on the control performance characteristics).

In test 1 the machine is driven at 500 rpm with no-load. When the multiphase drive reaches the steady state, all the switches of one phase (phase a in our case, S_{a1} and $\bar{S}_{a1}$) are forced to their OFF state at $t = 0.01\ s$, this being considered as an OPF fault. The implemented VSDFD method is running from the beginning of test 1, being all fault indices practically null before the OPF condition appears (see Fig. 6). This is a consequence of the control performance during the healthy operation, where x-y currents are successfully regulated to zero. After the OPF occurrence, the current of the faulty phase becomes zero and the fault index e_a increases. Notice however that the indices of the remaining healthy phases stay close to zero after the application of the OPF. In order to provide a security margin, a threshold for the fault detection is experimentally set to $T_{th} = 0.13$ considering the worst-case scenario in order to avoid false alarms. The definition of the security margin avoids false alarms and decreases the fault detection time down to 4 ms. The speed of detection is around 15% of the fundamental period T_f, which is roughly four times faster than the one obtained in well-known approaches [21].

The promising performance shown by VSDFD in test 1 must be however verified in common open-circuit faults that occur in the converter. Tests 2 and 3 are devoted to verify the performance of the proposed fault detection method in the event of an open-phase fault in the bottom (OSF1) and top (OSF2) power switches of one phase (phase a, in our case). The machine is again driven at 500 rpm but in this case with a load torque of 3.5 Nm. The load torque will increase the peak value of the phase currents but it does not affect the fault detection performance because the fault indices are normalized and the method does not depend on the operating point. Fig. 7 shows the fault indices in the transition from healthy to OSF1 operation (test 2). It is found again that the indices in the healthy phases are close to zero during the whole test, thus avoiding any false alarm. On the contrary, the index e_a starts to increase slightly after the OSF1 occurrence because the current is negative in phase a when OSF1 occurs (see zoom-in figure on the right side of Fig. 7). However, at time $t = 0.135\ s$ the current in phase a starts to flow in the positive direction because it can circulate though the healthy upper switch (S_{a1} in Fig. 1). In that moment the fault index is still below the threshold ($e_a = 0.015$ whereas $T_{th} = 0.13$) and consequently the fault is not detected yet. During half a fundamental period (from $t = 0.137$ to $0.154\ s$), the current in phase a evolves like in pre-fault operation and the fault index e_a is frozen at 0.015 (see zoom-in figure on the left side of Fig. 7). It is then necessary to wait until the current in phase a aims to be reversed and the OSF1 condition affects the system. At this moment the open-circuit in switch $\bar{S}_{a1}$ nullifies the phase current again and the fault index e_a continues rising, eventually surpassing the threshold at $t = 16s$. The detection time is now around 23 ms, which corresponds to the 67% of the fundamental period T_f (period

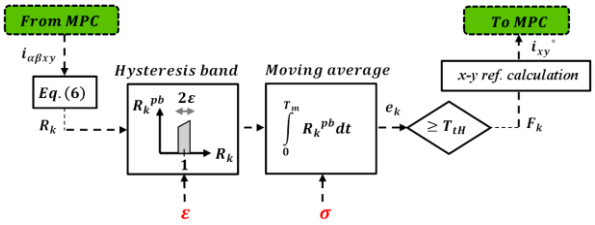

Fig. 4. Proposed fault detection scheme (see Fig. 2 to link with the model predictive control stage).

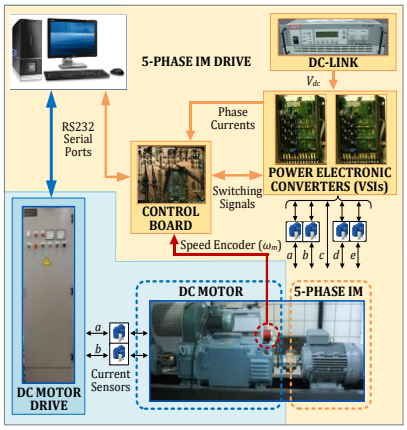

Fig. 5. Test bench.

TABLE I.
INDUCTION MACHINE PARAMETERS

Power (kW)	0.7
Torque (N · m)	6.27
n_m (rpm)	1000
i_d (A)	0.57
i_q (A)	2.50
R_s (Ω)	12.85
R_r (Ω)	4.80
L_m (mH)	681.70
L_{ls} (mH)	79.93
L_{lr} (mH)	79.93

of time that the VSDFD mechanism waited during the positive current cycle of the faulty phase plus a 17% of T_f, similarly to in test 1).

Test 3 verifies the fault detection when the top power switch remains in open-circuit (OSF2). In this type of fault, the situation is dual compared to OSF1, meaning that the current can flow during the negative part of the fundamental period and it is limited to zero in the positive part of the cycle (see Fig. 8). In test 3 the instant of the fault is more favorable than in test 2 since the current in phase a was about to become positive when the OSF2 is applied (see zoom-in figure on the right side of Fig. 8). This implies that the fault index e_a starts to rise almost immediately after the fault occurrence and its value exceeds that of the threshold before the current aims to become negative. At time $t = 0.16\ s$ the negative cycle in phase a allows the flow of the current through the bottom healthy switch ($\bar{S}_{a1}$ in Fig. 1), but at that moment the OSF2 situation has been already detected. The time of detection in this case is somewhat similar to that of the OPF, being 19% of the fundamental period ($4.75\ ms$). It must be highlighted however that the detection of the OSF2 is faster than OSF1 only in the specific conditions of both tests. In general, the speed of detection is dependent on the OSF instant, and in a worst-case scenario the speed of detection is similar to that of the OPF plus half the fundamental period (see test 2).

It can be observed that the fault index e_a presents additional ripple in OSFs compared to OPFs. This effect can be diminished by setting longer integration times in the moving average (i.e. higher values of σ), but this would in turn result in longer detection times, Since the margin of security is still sufficiently large, the speed of detection is promoted setting a value of $\sigma = 0.4$ in tests 1-3.

Tests 1 to 3 have verified the performance of the fault detection technique for single OPFs and OSFs, confirming that the fault indices from (6) can be equally used in both types of faults with success. Tests 4 confirms the capability of the method to detect multiple and simultaneous open-circuit faults. The case with concurrent OPFs in phases a and b is shown in Fig. 9a and the case with concurrent OSFs in phases a (top IGBT) and b (bottom IGBT) is shown in Fig. 9b. In both cases the indices of the faulty phases (a and b) start to rise after the fault occurrence and the remaining healthy indices remain close to zero. As in the previous tests this allows setting threshold that flags the faulty phases when surpasses (see zoom-in plots in Fig. 9a and 9b). The results in Fig. 9 further confirm that the VSDFD method can be used for single and multiple open-circuits faults including OPFs and OSFs.

A critical issue in fault detection methods is the avoidance of false alarms. Since fault indices are typically based on steady-state currents, transients might influence fault indices e_k and eventually provide a false alarm if the threshold is surpassed. Aiming to verify the robustness of the method, tests 5 and 6 drive the machine in dynamic conditions, for both transient speed and sudden load torque modes, respectively.

In test 5 the machine is driven from 500 to 300 rpm (left subplot in Fig. 10) causing a distortion of the phase currents (right subplot in Fig. 10). It is found however that the fault indices remain completely unaffected during the speed transient (main plot in Fig. 10). The reason for this is related to the definition of the fault indices e_k, which are based on ratios whose numerators include the *x*-*y* currents. Since the *x*-*y* currents are constantly regulated to zero in all dynamic conditions, the proposed fault indices in (6) will continue close to zero in all kind of transients as long as the regulation of the *x*-*y* currents is performed accurately.

In test 6 the machine is driven at 500 rpm with 3.5 Nm and the load is released at $t = 0.75\ s$, causing the transient that is shown in Fig. 11. Since the machine is healthy all throughout the test, all fault indices are kept close to zero and no false alarms appear. This test, together with that in Fig. 10 confirm the immunity of the VSDFD method against different transients.

Aiming to cover all cases that might be suspicious of bringing incorrect results, test 7 drives the machine at zero speed and verifies the capability of the VSDFD to identify and localize the fault in such condition. Even though the machine is driven at zero speed, it is still magnetized with a d-current equal to 0.57 A, hence the phase currents are non-null in pre-fault operation (See Fig. 12). An OPF in phase e is provoked at $t = 0.14s$ and this causes the fault index of phase e to immediately rise as in the cases shown in tests 1 to 4. The detection time is around $8\ ms$, which is roughly the same as in the previous tests. It is thus confirmed that the VSDFD method can also be applied at zero speed.

It has been shown so far that the VSDFD approach can successfully detect different kind of open-circuit faults (single and multiple OPF, OSF1 and OSF2) with good robustness and detection speed (even at zero speed). A final test 5 is performed to verify the impact of the fault detection delay on the drive performance when regulated using MPC. This test is specifically timely in the control strategy since the predictive approach is known to misbehave to select the switching states of the converter in the event of a fault, because it uses an incorrect model of the system. Test 7 drives the machine at 50 rpm with a load torque of 0.25 Nm when an OPF in phase a is applied at time $t = 0.2\ s$. Two different cases are considered at this instant: a fault detection delay of a fundamental period T_f (left plots in Fig. 12) and a fault detection delay of 15% of the fundamental period (right plots in Fig. 12). In both cases the control is reconfigured after the fault detection delay as explained in section III. The main aim of the test is to explore how critical is the fault detection delay in MPC-based schemes. Immediately after the fault occurrence the predictive model becomes highly inaccurate and the d-q currents cannot be tracked anymore (Fig. 10b). In the specific case of the OPF in phase a this only affects the α-current (Fig. 10c) because phase a does not contribute to the production of β-current due to its physical disposition. As a consequence of the poor current tracking during the fault detection, the control is lost and the speed drops (Fig. 10a). Once the fault is detected and the control is reconfigured, the machine speed is recovered, reaching again the pre-fault steady-state reference speed (it is assumed that the machine ratings are not exceeded in post-fault mode). It can be observed (see Fig. 10d) that the x-current is successfully tracked to the correct post-fault value (i.e. $i_x = -i_\alpha^*$) after the control is self-reconfigured. Fig. 10 makes it clear how MPC loses the control after the fault occurrence as well as the impact of the fault detection delay on the speed tracking. When operating at higher loads, this can eventually stop the machine.

Although a fault detection time of one fundamental period would be considered a fast detection for diagnosis purposes, it can lead to undesirable trasients and speed oscillations

when the aim is to have a self-reconfigurable fault-tolerant drive. Conversely, the reduction of the detection time to 15% of the fundamental period highly reduces the speed drop and provides a smooth transition from pre- to post-fault modes of operation.

The present work offers the following statements:

1. Although model predictive control can be considered a powerful strategy for electric drives, and many times has been described like a promising competitor of FOC methods, it misbehaves in the event of open-circuit faults.
2. The speed of detection of the fault is particularly critical in MPC-based drives in order to make a smooth transition from pre- to post-fault situations.
3. The proposed fault detection method (VSDFD) can detect and localize all kind of open-circuit faults, including both phase and swicth types. Though the fault indices depend on the number of phases, they can be easly redefined and extended for any multiphase machine with distributed windings. The same indices are used for fault detection and identification, this being mandatory in MPC in order to reconfigure the control strategy.
4. The proposed fault indices remain close to zero in all healthy phases both in pre- and post-fault situations, thus providing a good security margin to set the detection threshold. In addition, the zero value of *x-y* currents (compared to oscillating phase currents) allows the integration period of the moving average to be set below the fundamental period T_f. As a consequence, VSDFD provides a very short detection time, being in the range of 15% of the fundamental period (plus an extra 50% in the worst case scenario of switch faults).
5. The decoupling between *x-y* and α-β planes maintains the proposed fault indices at zero value in any dynamic condition, thus avoiding false alarms in transients and providing good robustness.
6. The VSDFD method is non-invasive, simple to implement and it does not depend on the drive parameters, operating point or control strategy.

VI. Conclusions

This work extends the fault detection strategy named VSDFD to five-phase electric drives that are controlled with one current harmonic using a model predictive control (MPC) strategy under all kind of open-circuit faults. Even though the MPC approach is known to misbehave in the event of open-circuit faults, the high speed of detection provided by the VSDFD allows a smooth and satisfactory transition from pre- to post-fault situations. At the same time, the decoupling of the x-y plane with the energy conversion process inherently provides good robustness and avoids false alarms. These advantageous features are verified in all kind of open-switch faults in the converter with redefined fault detection indices for five-phase systems. The results allow concluding that the VSDFD method can be easily generalized to any multiphase drive supplied with sinusoidal currents, regardless of the number of phases, control strategy and type of open-circuit fault.

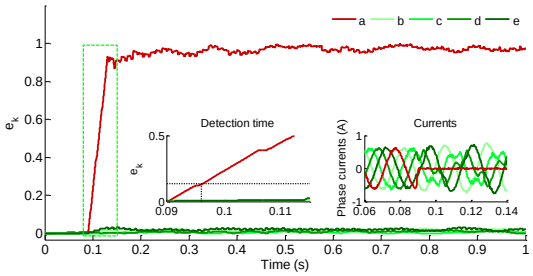

Fig. 6. Test 1 - Open-phase fault (OPF) in phase a. Evolution of the fault indices e_k (main plot) and zoom-in figures of the fault indices (left plot) and phase currents (right plot).

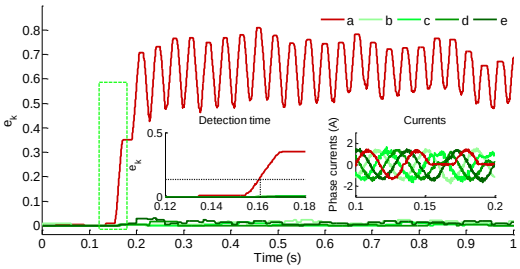

Fig. 7. Test 2 - Open-switch fault in the bottom IGBT (OSF1) of phase a. Evolution of the fault indices e_k (main plot) and zoom-in figures of the fault indices (left plot) and phase currents (right plot).

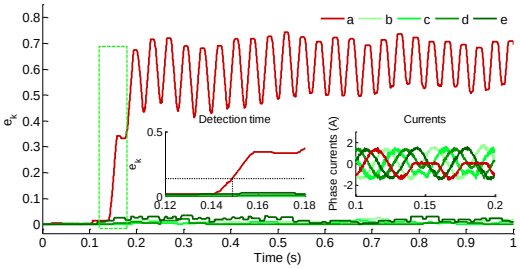

Fig. 8. Test 3 - Open-switch fault in the top IGBT (OSF2) of phase a. Evolution of the fault indices e_k (main plot) and zoom-in figures of the fault indices (left plot) and phase currents (right plot).

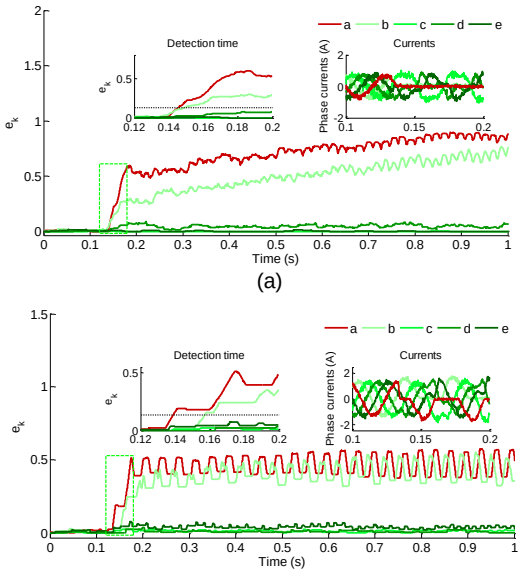

Fig. 9: Test 4 – Concurrent open-circuit faults in phases. (a) OPFs in phases *a* and *b*, and (b) OSFs in phases a (top IGBT) and b (bottom IGBT). Evolution of the fault indices e_k (main plot) and zoom-in figures of the fault indices (left plot) and phase currents (right plot).

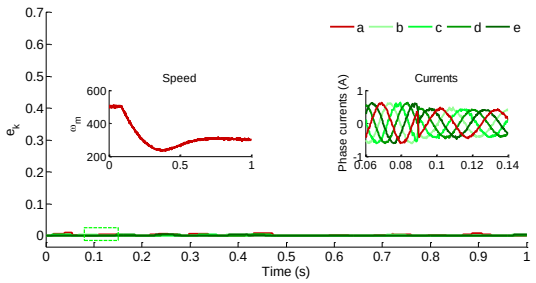

Fig. 10. Test 5 - Speed transient in healthy operation. Evolution of the fault indices e_k (main plot) and zoom-in figures of the speed (left plot) and phase currents (right plot) during a speed transient.

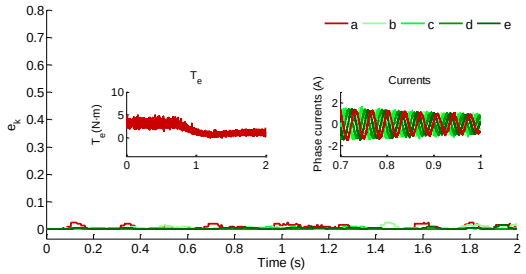

Fig. 11. Test 6 – Sudden load torque transient in healthy operation. Evolution of the fault indices e_k (main plot) and zoom-in figures of the speed (left plot) and phase currents (right plot) during a load torque transient.

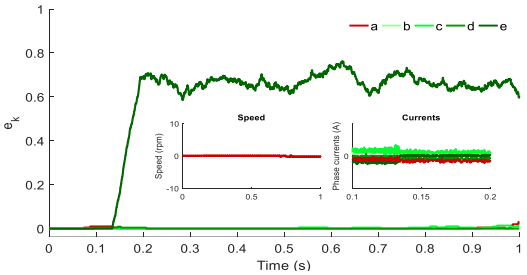

Fig. 12. Tests 7 – Open-phase fault in phase e at zero speed. Evolution of the fault indices e_k (main plot) and zoom-in figures of the speed (left plot) and phase currents (right plot) during the test.

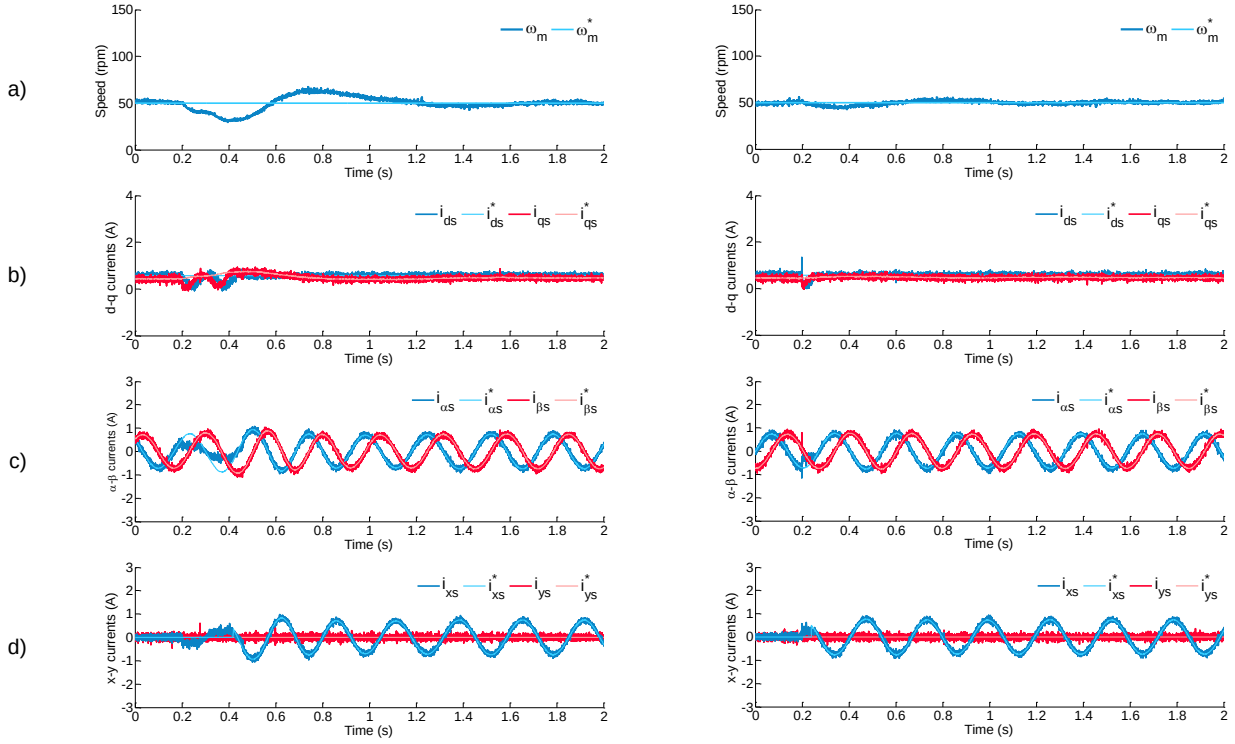

Fig 13. Test 8 - Transition from pre- to post-fault situation with MPC with fault detection delays of a fundamental period T_m (left plots) and a 15% of the fundamental period (right plots). From top to bottom: a) Motor speed, b) d-q currents, c) α-β currents and d) x-y currents.

REFERENCES

[1] E. Levi, F. Barrero and M.J. Duran, "Multiphase machines and drives – Revisited," *IEEE Trans. Ind. Electron.*, vol 63, no. 1, pp. 429-432, 2016.

[2] E. Levi, "Advances in converter control and innovative exploitation of additional degrees of freedom for multiphase machines," *IEEE Trans. on Ind. Electron.*, vol 63, no. 1, pp. 433-448, 2016.

[3] F. Barrero and M.J. Duran, "Recent advances in the design, modeling and control of multiphase machines – Part 1," *IEEE Trans. on Ind. Electron.*, vol 63, no. 1, pp. 449-458, 2016.

[4] M.J. Duran and F. Barrero, "Recent advances in the design, modeling and control of multiphase machines – Part 2," *IEEE Trans. on Ind. Electron.*, vol 63, no. 1, pp. 459-468, 2016.

[5] E. Jung, H. Yoo, S. Sul, H. Choi and Y. Choi, "A nine-phase permanent-magnet motor drive system for an ultrahigh-speed elevator," *IEEE Trans. on Ind. Appl.*, vol. 48, no. 3, pp. 987-995, 2012.

[6] V. Yaramasu, A. Dekka, M.J. Duran, S. Kouro and B. Wu, "Permanent magnet synchronous generator-based wind energy conversion systems: Survey on Power Converters and Controls," *IET Electric Power Appl.*, DOI: 10.1049/iet-epa.2016.0799, Early Access, 2017.

[7] A. Cavagnino, Z. Li, A. Tenconi and S. Vaschetto, "Integrated generator for more electric engine: design and testing of a scaled-size prototype," *IEEE Trans. Ind. Appl.*, vol. 49, no. 5, pp. 2034-2043, 2013.

[8] G. Sulligoi, A. Tessarolo, V. Benucci, A.M. Trpani, M. Baret and F. Luise, "Shipboard Power Generation: Design and Development of a Medium-Voltage dc Generation System," *IEEE Ind. Appl. Mag.*, vol. 19, no. 4, pp. 47-55, 2013.

[9] J. Rodriguez, R.M. Kennel, J.R. Espinoza, M. Trincado, C.A. Silva and C.A. Rojas, "High-Performance Control Strategies for Electrical Drives: An Experimental Assessment," *IEEE Trans. on Ind. Electron.*, vol. 59, no. 2, pp. 812-820, 2012

[10] E. Fuentes, D. Kalise, J. Rodríguez and R.M. Kennel, "Cascade-Free Predictive Speed Control for Electrical Drives," *IEEE Trans. Ind. Electron.*, vol. 61, no. 5, pp. 2176-2184, 2014.

[11] C. Lim, E. Levi, M. Jones, N. Abd Rahim and W. Hew, "FCS-MPC Based Current Control of a Five-Phase Induction Motor and its Comparison with PI-PWM Control," *IEEE Trans. on Ind. Electron.*, vol. 61, no. 1, pp. 149-163, 2014.

[12] J. Riveros, F. Barrero, E. Levi, M.J. Durán, M. Jones and S. Toral, "Variable-Speed Five-Phase Induction Motor Drive Based on Predictive Torque Control," *IEEE Trans. on Ind. Electron.*, vol. 60, no. 8, pp. 2957-2968, 2013.

[13] M. Salehifar, M. Moreno-Eguilaz, G. Putrus, P. Barras, “Simplified fault tolerant finite control set model predictive control of a five-phase inverter supplying BLDC motor in electric vehicle drive,” *Elsevier Electric Power System Research*, vol. 132, pp. 56-66, 2016.

[14] C. Martín, M.R. Arahal, F. Barrero and M.J. Duran, “Five-Phase Induction Motor Rotor Current Observer for Finite Control Set Model Predictive Control of Stator Current,” *IEEE Trans. on Ind. Electron.*, vol. 63, no. 7, pp. 4527-4538, 2016.

[15] B. Bogado, F. Barrero, M.R. Arahal, S. Toral, E.Levi “Sensitivity to electrical parameter variations of Predictive Current Control in multiphase drives,” *in proc. of IECON 2013 - 39th Annual Conference of the IEEE Industrial Electronics Society*, pp. 5215-5220, Vienna, Austria, 2013.

[16] H. Guzmán, M.J. Duran, F. Barrero, B. Bogado and S. Toral, “Speed control of five-phase induction motors with integrated open-phase fault operation using model-based predictive current control techniques,” *IEEE Trans. on Ind. Electron.*, vol. 61, no. 9, pp. 4474-4484, 2014.

[17] H. Guzman, M.J. Duran, F. Barrero, L. Zarri, B. Bogado, I. Gonzalez-Prieto and M.R. Arahal, “Comparative Study of Predictive and Resonant Controllers in Fault-Tolerant Five-phase Induction Motor Drives,” *IEEE Trans. on Ind. Electron.*, vol. 63, no. 1, pp. 606-617, 2016.

[18] C. Martín, M. R. Arahal, F. Barrero and M. J. Durán, "Five-Phase Induction Motor Rotor Current Observer for Finite Control Set Model Predictive Control of Stator Current," *IEEE Trans. on Ind. Electron.*, vol. 63, no. 7, pp. 4527-4538, July 2016.

[19] H. Henao, G.A. Capolino, M. Fernandez-Cabanas, F. Filippetti, C. Bruzzese, E. Strangas, R. Pusca, J. Estima, M. Riera-Guasp and S. Hedayati-Kia , “Trends in Fault Diagnosis for Electrical Machines: A Review of Diagnostic Techniques,” *IEEE Ind. Electron Magaz.*, vol 8, no. 2, pp. 31-42, 2014.

[20] M. Riera-Guasp, J.A. Antonino-Daviu, and G.A. Capolino “Advances in Electrical Machine, Power Electronic, and Drive Condition Monitoring and Fault Detection: State of the Art,” *IEEE Trans. on Ind. Electron.*, vol. 62, no. 3, pp. 1746-1759, 2015.

[21] M.J. Duran, I. Gonzalez-Prieto, N. Rios and F. Barrero, “A Simple, Fast and Robust Open-phase Fault Detection Technique for Six-phase Induction Motor Drives,” *IEEE Trans. on Ind. Electron.*, DOI: 10.1109/TPEL.2017.2670924, Early Access, 2017.

[22] J. O. Estima and A. J. M. Cardoso, “A new approach for real-time multiple open-circuit fault diagnosis in voltage source inverters,” *IEEE Trans. Ind. Applicat.*, vol. 47, no. 6, pp. 2487–2494, 2011.

[23] N. M. A. Freire, J. O. Estima, and A. J. M. Cardoso, “Open-circuit fault diagnosis in PMSG drives for wind turbine applications,” *IEEE Trans. Ind. Electron.*, vol. 60, no. 9, pp. 3957–3967, 2013.

[24] W. Sleszynski, J. Nieznanski, and A. Cichowski, “Open-transistor fault diagnostics in voltagesource inverters by analyzing the load currents,” *IEEE Trans. Ind. Electron.*, vol. 56, no. 11, pp. 4681–4688, 2009.

[25] J. O. Estima and A. J. M. Cardoso, “A new algorithm for real-time multiple open-circuit fault diagnosis in voltage-fed PWM motor drives by the reference current errors,” *IEEE Trans. Ind. Electron.*, vol. 60, no. 8, pp. 3496–3505, 2013.

[26] L. Zarri, M. Mengoni, Y. Gritli, A. Tani, F. Filippetti, G. Serra and D. Casadei, “Detection and localization of stator resistance dissymmetry based on multiple reference frame controllers in multiphase induction motor drives,” *IEEE Trans. Ind. Electron.*, vol. 60, no. 8, pp. 3506-3518, 2013.

[27] M. Trabelsi, E. Semail, N. K. Nguyen and F. Meinguet, “Open-switch and open-phase real time FDI process for multiphase PM Synchronous Motors,” 2016 IEEE 25th International Symposium on Industrial Electronics (ISIE), Santa Clara, CA, 2016, pp. 179-185.

[28] M. Trabelsi, N. K. Nguyen and E. Semail, “Real-Time Switches Fault Diagnosis Based on Typical Operating Characteristics of Five-Phase Permanent-Magnetic Synchronous Machines,” *IEEE Trans. on Ind. Electron.*, vol. 63, no. 8, pp. 4683-4694, Aug. 2016.

[29] M. Salehifar, R. S. Arashloo, J. M. Moreno-Equilaz, V. Sala and L. Romeral, "Fault Detection and Fault Tolerant Operation of a Five Phase PM Motor Drive Using Adaptive Model Identification Approach," *IEEE Journal of Emerging and Selected Topics in Power Electronics*, vol. 2, no. 2, pp. 212-223, June 2014.

[30] Arafat; S. Choi; J. Baek, "Open Phase Fault Detection of a Five-Phase Permanent Magnet Assisted Synchronous Reluctance Motor based on Symmetrical Components Theory," *IEEE Trans. on Ind. Electron.*, DOI. 10.1109/TIE.2017.2682016

[31] Y. Fan, C. Li, W. Zhu, X. Zhang, L. Zhang and M. Cheng, "Stator Winding Interturn Short-Circuit Faults Severity Detection Controlled by OW-SVPWM Without CMV of a Five-Phase FTFSCW-IPM," *IEEE Trans. on Ind. Applicat.*, vol. 53, no. 1, pp. 194-202, Jan.-Feb. 2017.

[32] R. Hu, J. Wang, B. Sen, A. R. Mills, E. Chong and Z. Sun, "PWM Ripple Currents Based Turn Fault Detection for Multiphase Permanent Magnet Machines," *IEEE Trans. on Ind. Applicat.*, vol. 53, no. 3, pp. 2740-2751, May-June 2017.

[33] B. Sen and J. Wang, "Stator Interturn Fault Detection in Permanent-Magnet Machines Using PWM Ripple Current Measurement," *IEEE Trans. on Ind.l Electron.*, vol. 63, no. 5, pp. 3148-3157, May 2016.

[34] S. Choi, M. S. Haque, A. Arafat and H. A. Toliyat, "Detection and Estimation of Extremely Small Fault Signature by Utilizing Multiple Current Sensor Signals in Electric Machines," *IEEE Trans. on Ind. Applicat.*, vol. 53, no. 3, pp. 2805-2816, May-June 2017.

[35] M. Salehifar, R. Salehi Arashloo, M. Moreno-Eguilaz, V. Sala and L. Romeral, "Observer-based open transistor fault diagnosis and fault-tolerant control of five-phase permanent magnet motor drive for application in electric vehicles," *IET Power Electron.*, vol. 8, no. 1, pp. 76-87, 1 2015.

[36] M. Bermudez, I. Gonzalez-Prieto, F. Barrero, H. Guzman, X. Kestelyn and M. Duran, “An Experimental Assessment of Open-Phase Fault-Tolerant Virtual Vector Based Direct Torque Control in Five-Phase Induction Motor Drives,” *IEEE Trans. on Power Electron.*, DOI: 10.1109/TPEL.2017.2711531.

[37] M. Bermudez, I. Gonzalez-Prieto, F. Barrero, H. Guzman, M.J. Duran, X. Kestelyn, “Open-Phase Fault-Tolerant Direct Torque Control Technique for Five-Phase Induction Motor Drives,” *IEEE Trans. Ind. Electron., early access*, 2016.

[38] H.S. Che, M.J. Duran, E. Levi, M. Jones, W.P. Hew and N.A. Rahim, “Post-fault operation of an asymmetrical six-phase induction machine with single and two isolated neutral points,” *IEEE Trans. on Power Electron.*, vol. 29, no. 10, pp. 5406-5416, 2014.

[39] A. Mohammadpour and L. Parsa, “Global fault-tolerant control technique for multi-phase permanent-magnet machines,” *IEEE Trans. Ind. Appl.*, vol. 51, no. 1, pp. 178-186, 2015.

[40] A.S. Abdel-Khalik, M.A. Elgenedy, S. Ahmed and A.M. Massoud, “An improved fault-tolerant five-phase induction machine using a combined star/pentagon ingle layer stator winding connection,” *IEEE Trans. Ind. Electron.*, vol. 63, no. 1, pp. 618-628, 2016.

[41] A. Tani, M. Mengoni, L. Zarri, G. Serra and D. Casadei, “Control of multiphase induction motors with an odd number of phases under open-circuit phase faults,” *IEEE Trans. Power Electron.*, vol. 27, no. 2, pp. 565-577, 2012.

[42] M. Taherzadeh , S. Carriere, F. Betin, M. Joorabian, R. Kianinezhad and G.A. Capolino, “A Novel Strategy for Sensorless Control Modification of a Six-phase Induction Generator in Faulted Mode,” *Electric Power Compon. and Systems*, vol. 44, no. 8, pp. 941-953, 2016.

[43] I. Gonzalez-Prieto, M.J. Duran and F. Barrero, “Fault-tolerant Control of Six-phase Induction Motor Drives with Variable Current Injection,” *IEEE Trans. Power Electron.*, DOI: 10.1109/TPEL.2016.2639070, Early Acess, 2016.

[44] M. Salehifar, R. S. Arashloo, M. Moreno-Eguilaz, V. Sala and L. Romeral “Observer-based open transistor fault diagnosis and fault-tolerant control of five-phase permanent magnet motor drive for application in electric vehicles,” *IET Power Electron.*, vol. 8, no. 1, pp. 76-87, 2015.

[45] WNWA Munim, M. J. Duran, H. S. Che, M. Bermudez, I. Gonzalez-Prieto and N. A. Rahim, “A Unified Analysis of the Fault Tolerance Capability in Six-phase Induction Motor Drive,” *IEEE Trans. on Power Electron.*, DOI: 10.1109/TPEL.2016.2632118.

[46] Y. Zhao and T. A. Lipo, “Space vector PWM control of dual three-phase induction machine using vector space decomposition,” *IEEE Trans. on Ind. Appl.*, vol. 31, no. 5, pp. 1100–1109, Sep./Oct. 1995.

[47] M. J. Duran, J. A. Riveros, F. Barrero, H. Guzman and J. Prieto, "Reduction of common-mode voltage in five-phase induction motor drives using predictive control techniques," *IEEE Trans. on Ind. Appl.*, vol. 48, no. 6, pp. 2059-2067, Nov.-Dec. 2012.

[48] A. Yepes, J.A. Riveros, J. Doval-Gandoy, F. Barrero, O. Lopez, B. Bogado, M. Jones, E. Levi, "Parameter identification of multiphase induction machines with distributed windings-part 1: sinusoidal excitation methods," *IEEE Trans. on Energy Conv.*, vol. 27, no. 4, pp. 1056-1066, 2012.

[49] J.A. Riveros, A. Yepes, F. Barrero, J. Doval-Gandoy, B. Bogado, O. Lopez, M. Jones, E. Levi, "Parameter identification of multiphase induction machines with distributed windings-part 2: time-domain techniques," *IEEE Trans. on Energy Conv.*, vol. 27, no. 4, pp. 1067-1077, 2012.

Ignacio González Prieto was born in Malaga, Spain, in 1987. He received the Industrial Engineer and M.Sc. degrees in fluid mechanics from the University of Malaga, Malaga, Spain, in 2012 and 2013, respectively, and the Ph.D. degree in electronic engineering from the University of Seville, Sevilla, Spain, in 2016. His research interests include multiphase machines, wind energy systems, and electrical vehicles.

Mario J. Duran was born in Malaga, Spain, in 1975. He received the M.Sc. and Ph.D. degrees in electrical engineering from the University of Malaga, Malaga, in 1999 and 2003, respectively. He is currently an Associate Professor in the Department of Electrical Engineering, University of Malaga. His research interests include modeling and ´ control of multiphase drives and renewable energies conversion systems.

Natalia Rios-Garcia was born in Malaga, Spain, in 1993. She received the Industrial Engineer degree from the University of Malaga, Spain, in 2016. She is actually a student of a M. Sc in the University of Malaga, Spain. Her research interests include multiphase machines, fault detection methods, wind energy systems and electrical vehicles.

Federico Barrero (M 04; SM 05) received the MSc and PhD degrees in Electrical and Electronic Engineering from the University of Seville, Spain, in 1992 and 1998, respectively. In 1992, he joined the Electronic Engineering Department at the University of Seville, where he is currently a Full Professor. He received the Best Paper Awards from the IEEE Trans. on Ind. Electron. for 2009 and from the IET Electric Power Applications for 2010-2011.

Cristina Martín was born in Seville, Spain, in 1989. She received the Industrial Engineer degree from the University of Málaga, Spain, in 2014. In 2015, she joined the Electronic Engineering Department of the University of Seville, where she is currently working toward the Ph.D. degree. Her current research interests include modeling and control of multiphase drives, microprocessor and DSP device systems, and electrical vehicles.